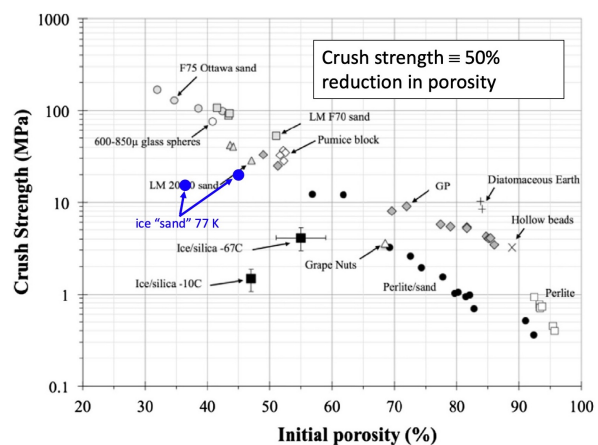


**COMPACTION CRATERS IN THE KUIPER BELT: IMPLICATIONS FOR KBO SIZE-FREQUENCY DISTRIBUTIONS AND SURFACE COMPOSITION AND STRUCTURE.** William B. McKinnon<sup>1</sup>, K.N. Singer<sup>2</sup>, S.J. Robbins<sup>2</sup>, X. Mao<sup>1</sup>, P.M. Schenk<sup>3</sup>, O.L. White<sup>4,5</sup>, J.R. Spencer<sup>2</sup>, W.M. Grundy<sup>6,7</sup>, J.M. Moore<sup>5</sup>, S.A. Stern<sup>2</sup>, H.A. Weaver<sup>8</sup>, C.B. Olkin<sup>2</sup>, and the *New Horizons* Science Team; <sup>1</sup>Dept. Earth and Planetary Sci. and McDonnell Center for the Space Sci., Washington University in St. Louis, Saint Louis, MO 63130 (mckinnon@wustl.edu), <sup>2</sup>Southwest Research Institute, Boulder, CO 80302, <sup>3</sup>LPI, Houston, TX 77058, <sup>4</sup>SETI Inst., Mountain View, CA 94043, <sup>5</sup>NASA Ames Res. Center, Moffett Field, CA 94035, <sup>6</sup>Lowell Observatory, Flagstaff, AZ 86001, <sup>7</sup>Dept. Astronomy and Planetary Sci., NAU, Flagstaff, AZ 86011, <sup>8</sup>JHUAPL, Laurel, MD 20723.

**Introduction:** The slow spin of cold classical Kuiper belt object (CCKBO) Arrokoth as well as its gravitational surface slope distribution and structural integrity suggest that it is a remarkably low-density body,  $\sim 250$  to  $500 \text{ kg m}^{-3}$  [1-6]. Such a density is similar to the lower end of estimates for cometary nuclei (with which Arrokoth likely shares a similar formation history [7,8]), though lower than that of 67P/Churyumov-Gerasimenko,  $532 \pm 7 \text{ kg m}^{-3}$  [9]. For example, comet 9P/Tempel 1 has a preferred density range from 200 to  $470 \text{ kg m}^{-3}$ , from non-gravitational force (NGF) and *Deep Impact* ejecta plume modeling; from NGF modeling, 19P/Borrelly has a preferred density of  $490 \text{ kg m}^{-3}$ , whereas for 81P/Wild 2 this value is  $300 \text{ kg m}^{-3}$  (see Table 1 in [9]). Bulk densities between 250 and  $500 \text{ kg m}^{-3}$  imply substantial porosities ( $>70\%$ ) for both cometary and Arrokoth's presumed ice+refractory dust compositions [10,11]. This inference is supported by direct porosity estimates from CONSORT microwave sounding of the interior 67P,  $\sim 75\text{-}85\%$  [9].

When the porosity of a surface is high enough (above the usual close packing thresholds for granular materials of 30-40%) and when the crushing strength ( $Y_c$ ) low enough, impact craters can form partially or wholly by compaction as opposed to excavation and displacement [12,13]. Limited experimental evidence shows that the  $Y_c$  for cold (77 K), granular ice [14] and porous ice-silicate mixtures [15] are lower than those for siliceous materials such as pumice at the same porosity (Fig. 1), although no experiments have been carried out on ice-rock(-organic) mixtures at the large porosities ( $\gtrsim 70\%$ ) likely appropriate to comets, Arrokoth, and other small KBOs. Because the transition to compaction cratering occurs when  $\rho g H \gtrsim 0.005 Y_c$ , where  $\rho$  is density,  $g$  is surface gravity, and  $H$  is crater depth [13], even  $Y_c \sim 25\text{-}100 \text{ kPa}$  (plausible from Fig. 1) brings the 7-km wide Sky impact (Arrokoth's largest known) to the compaction cratering threshold. If bulk Arrokoth has the crush strength of fresh snow ( $< \text{few kPa}$ , e.g., Fig. 10 in [16]), then all its identified craters formed by compaction.

The implications of compaction cratering for Arrokoth and other small KBOs are multiple [17]: 1) suppression of impact ejecta leads to momentum “ $\beta$ ”



**Fig. 1. Crush strength of various granular aggregates as a function of porosity.** The crush strength for highly porous, icy KBOs such as Arrokoth is plausibly well under 1 MPa. From [13] with ice “sand” points from [14].

values closer to unity; 2) crater scaling depends on both porosity and a strength measure ( $Y_c$ ); 3) crush up concentrates thermal effects near and below craters, leading to surface devolatilization and armoring; 4) crush up protects small KBOs from catastrophic disruption; and 5) for Arrokoth and other contact binary KBOs, it stabilizes the join between lobes (e.g., we find the formation of Sky likely broke Arrokoth's neck, but it mended). Here we focus on points (2) and (3).

**Scaling:** Crater scaling for *highly porous* granular materials (those with porosities  $n$  greater than 50%) is given by Eq. (20) in [13]:

$$\pi_V = \left[ 0.75 \left( \frac{Y_c}{\rho U^2} \right)^{-3\mu/2} + 0.023 \pi_2^{-3\mu/(2+\mu)} \right] \times \text{psf}(n)$$

where  $\pi_V \equiv \rho V/m$  is cratering efficiency and  $\pi_2 \equiv ga/U^2$  the gravity-scaled size, with  $a$ ,  $m$ , and  $U$  the impactor radius, mass, and vertical velocity, respectively, and  $V$  the resulting crater volume (equal densities for impactor and target are assumed). The exponent  $\mu$  in this scaling is 0.54, and  $\text{psf}(n) = 10.4 \exp(-5.07n)$  is an empirical porosity scale factor derived by [13] from centrifuge impact experiments. We assume  $n$  varies linearly from 0.70 to 0.85 for bulk densities between 500 and  $250 \text{ kg m}^{-3}$ , respectively, and illustrate this scaling in Fig. 2 for a  $Y_c$  low enough so that com-

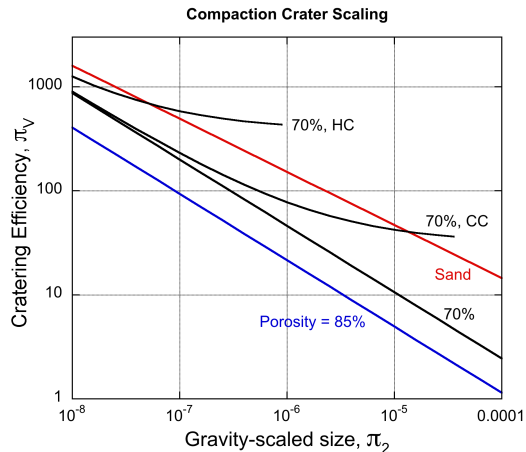


**Fig. 2. Cratering efficiency comparison between cohesionless regolith (modeled as dry sand) and highly porous granular materials,** based on [13]. High porosity lowers cratering efficiency (reduces mass excavated and displaced). Depending on the value of  $Y_c/\rho U^2$ , crushing and compaction can contribute to crater volume at larger gravity-scaled sizes, counteracting this trend. Such scaling is illustrated for  $Y_c = 100$  kPa,  $\rho = 500$  kg m<sup>-3</sup>, and the characteristic impact speeds for cold classical and hot classical Kuiper belt objects onto Arrokoth, 300 and 1400 m s<sup>-1</sup>, respectively [18]. The transition to compaction cratering is truncated here at its limit of applicability at right (see [13]).

paction scaling is achieved for Sky on Arrokoth, but not out of line with values in Fig. 1. Compaction scaling is a form of strength scaling, but in this case the strength asymptotes occur at large, rather than small,  $\pi_2$ .

**SFD Controversies.** The size-frequency distribution (SFD) for smaller KBO craters was measured directly on the unsaturated, ideally illuminated Charon cryovolcanic plain, “Vulcan” Planitia (VP). Least-squares fits and maximum likelihood estimates (MLE) in [19] give shallow differential power-law slopes near  $-1.7$  or  $-1.8$ ; MLE on remapped VP craters gives slightly steeper slopes near  $-2.0$  [20] (both papers quote slope uncertainties of 0.2–0.3). In contrast, [21] present a rather torturous series of arguments based on Arrokoth data that the VP crater differential SFD is actually  $-2.2$ -to- $-2.5$ , despite its clear incompatibility with the actual VP impact record.

Moreover, for Charon the crater SFD implies an even shallower *impactor* SFD [22]. For a more-or-less solid cryovolcanic surface and gravity scaling [23], the power-law slopes in [19,20] above translate to  $-1.3$ – $-1.4$  for simple craters,  $-1.5$ – $-1.6$  for complex. But for compaction scaling (on Arrokoth) the impactor SFD should be much closer to the crater SFD, i.e.,  $\pi_V$  is less dependent on  $\pi_2$  (Fig. 2), accentuating the disagreement between [19,20] and [21]. We note that [24] find that a differential crater SFD of  $-1.66 \pm 0.3$  is *not* incompatible with Arrokoth’s cratering record: the formation of a singular, large crater (Sky) may appear

improbable, but it can’t be statistically rejected. We also note that VP is by definition a resurfaced unit and while ancient [25] may not be quite as old a counting surface as Arrokoth, i.e., may or may not reflect the high, post-instability bombardment advocated by [21]. Or it may simply be that the impact crater population on Arrokoth, which is by no means as well characterized as that on VP [2,26], offers greater latitude in interpretation than argued in [21].

**Surface Densification and Heating.** Compaction (crush-up) implies that most of a given impactor’s kinetic energy is taken up as waste heat below the impact point, with momentum transferred to the rest of the body by elastic waves. For typical cold classical encounter velocities, impactor and near-field target temperatures should reach  $\sim 100$  K, warm enough to mobilize hypervolatile ices, whereas faster, hot classical or scattered disk objects can melt methanol and water ice. Stratigraphically, compaction craters consist of a densified lens buried by infilled loose surface material [13]. In contrast to a body like the Moon, where a volcanic surface can develop a fragmental surface layer or regolith under prolonged bombardment, a small underdense, granular KBO such as Arrokoth can develop a degree of (subsurface) armoring if sufficiently impacted. Arrokoth’s crater density is far from saturated [2], but if [21] is correct, then it and other “pristine” CCKBOs may be saturated by meter-scale impactors, which may partially account for its smooth appearance.

**Acknowledgements:** This research supported by NASA’s *New Horizons* project through contracts NASW-02008 and NAS5-97271/TaskOrder30.

**References:** [1] Stern S.A. et al. (2019) *Science* 364, eaaw9771. [2] Spencer J.R. et al. (2020) *Science* 367, eaay3999. [3] McKinnon W.B. et al. (2020) *Science* 367, eaay6620. [4] Keane J.T. et al. (2021) *JGR Planets*, submitted. [5] Hirabayashi M. et al. (2020) *ApJ Lett.* 891, L12. [6] Mao X. et al. (2021) *JGR Planets* 126, e2021JE006961. [7] Nesvorný D. (2018) *ARAA* 56, 137–174. [8] Morbidelli A. and Nesvorný D. (2020) in *The Trans-Neptunian Solar System*, 25–59, Elsevier. [9] Groussin O. et al. (2019) *SSR* 215, 29. [10] Grundy W.M. et al. (2020) *Science* 367, aay3750. [11] Mumma M.J. and Charnley S.B. (2011) *ARAA* 49, 471–524. [12] Collins G.S. et al. (2019) in *Shock Phenomena in Granular and Porous Materials*, Springer. [13] Housen K.R. et al. (2018) *Icarus* 300, 72–96. [14] Durham W.B. et al. (2005) *GRL* 32, L18202. [15] Yasui M. and Arakawa M. (2009) *JGR* 114, E09004. [16] Wang E. et al. (2021) *Cold Reg. Sci. Tech.* 182, 103215 [17] McKinnon W.B. et al., submitted. [18] Greenstreet S. et al. (2019) *ApJ Lett.* 872, L5. [19] Singer K.N. et al. (2019). *Science* 363, 955–959. [20] Robbins S.J. and Singer K.N. (2021) *PSJ* 2, 192. [21] Morbidelli A. et al. (2021) *Icarus* 356, 114256. [22] Singer K.N. et al. (2021) in *The Pluto System After New Horizons*, UA Press. [23] Housen K.R. and Holsapple K. A. (2011) *Icarus* 211, 856–875. [24] Robbins S.J. et al. (2021) *GRL* 48, e2021GL093247. [25] Moore J.M. and McKinnon W.B. (2021) *AREPS* 49, 173–200. [26] Schenk P. et al. (2021) *Icarus* 356, 113834.